UDC 551.509.313 : 551.511.32 : 532.5

NUMERICAL INTEGRATION OF FLUID FLOW OVER TRIANGULAR GRIDS

DAVID WILLIAMSON

Massachusetts Institute of Technology, Cambridge, Mass.

and

National Center for Atmospheric Research, Boulder, Colo.

ABSTRACT

Discrete approximations to hyperbolic partial differential equations governing frictionless two-dimensional fluid flow are developed in Cartesian geometry for use over arbitrary triangular grids. A class of schemes is developed that conserves mass, momentum, and total energy. The terms of the governing equations are also approximated individually and their truncation error is examined. For test integrations, the schemes are applied to an equilateral triangular (homogeneous) grid on a beta plane. In one case, the same scheme is integrated over a square grid for comparison between four- and six-point differences. Both second- and fourth-order schemes are integrated and compared with a fine resolution solution.

1. INTRODUCTION

The spatial scale of many geophysical fluid dynamics problems varies greatly over the domain of interest. The ocean circulation is such a problem. Western boundary currents such as the Gulf Stream or Kuroshio have a smaller scale than the remaining ocean circulation. Another example is the problem of fronts in the atmosphere, where relatively strong gradients exist in a narrow band with weak gradients elsewhere.

In order to study these problems numerically, a net of points must be defined over the domain. The density of the net must be great enough to resolve the smallest scales of interest. The size and speed of present computers do not allow a uniformly fine grid over the entire domain. Even if it were practical, such a grid would be inefficient since a fine grid is needed only over a small part of the domain. For efficient use of the computer, it seems reasonable to use the optimum grid density for the spatial scale of the expected solution in each part of the domain. These various density grids must then be connected to each other in some manner and, in some cases, special difference equations must be designed for use at the interface.

If a coarse square grid is joined to a fine square grid, various difficulties can arise at the interface. For example, if a uniform wave is traveling parallel to the interface, the phase truncation error is smaller in the fine grid than in the coarse one, and a shearing soon develops in the wave structure. This numerical phenomenon is exhibited in the case of a wave on a sphere by Gates and Riegel (1962). If a wave is moving in a direction perpendicular to the interface, partial reflections might occur which are due solely to the numerical techniques and not to the physical problem.

To avoid these problems, a nonhomogeneous triangular grid seems ideal. Such grids have been used successfully for solving elliptic equations by the method of successive overrelaxation (Winslow, 1966). They permit a continuous, gradual transition from fine to coarse grid and permit construction of secondary polyhedral grid areas whose sides are common to only two such areas.

Numerical integration over a sphere provides another use for triangular grids. Uniform grids over a sphere would be useful for atmospheric general circulation models. Quasi-homogeneous triangular grids have been defined over a sphere by Vestine et al. (1963) and Williamson (1968). Sadourny et al. (1968) and Williamson (1968) have integrated the nondivergent barotropic vorticity equation over these spherical grids.

Masuda (1968) has developed finite-difference schemes using the principle developed by Arakawa (1966) for use over a homogeneous triangular grid. He shows good results for integrations of the nondivergent barotropic model on a plane. Lorenz (1967) has developed a triangular finite-difference approximation for a two-level model on a beta plane when the governing equations are written in terms of a stream function. In the following, discrete approximations to the primitive equations governing frictionless two-dimensional flow are developed for use over arbitrary triangular grids. Cartesian geometry is assumed for this study. The modifications necessary for spherical geometry will be discussed in another paper. Two approaches are considered. The first deals with the invariants of the continuous equations. A class of schemes is developed that conserves mass, momentum, and energy. The second approach approximates each term of the governing equations individually and examines the truncation error of all the schemes when applied to a homogeneous grid over a plane.

Results of test integrations of these schemes are then presented. The schemes are applied to an equilateral triangular (homogeneous) grid on a beta plane. No integrations over nonhomogeneous grids are performed. The results of the triangular schemes are compared with results of similar schemes applied to a square net and with results of integrations over a fine mesh.

2. GOVERNING EQUATIONS

The equations considered here are those for frictionless horizontal two-dimensional motion. For the derivation of the difference schemes, the Coriolis term will be neglected. Since all quantities will be defined at the same grid points, the Coriolis term can be differenced in a straightforward manner. Using vector notation, the governing equations can be written.

$$\frac{\partial \mathbf{V}}{\partial t}+\mathbf{V}\cdot\nabla\mathbf{V}+g\nabla h=0 \tag{1}$$

and

$$\frac{\partial h}{\partial t}+\nabla\cdot(h\mathbf{V})=0 \tag{2}$$

where $\mathbf{V}$ is the vector velocity, h is the height of the free surface, g is gravity, and ∇ is the vector gradient operator. Equation (2) expresses conservation of mass.

The momentum equation can be formed from equations (1) and (2); and, using diadic notation, can be written as

$$\frac{\partial h\mathbf{V}}{\partial t}+\nabla\cdot(\mathbf{V}h\mathbf{V})+\nabla\left(g\frac{h^2}{2}\right)=0. \tag{3}$$

Thus, neglecting boundary effects, the system conserves momentum when integrated over the domain. The kinetic energy equation is obtained by combining equation (1) multiplied by $h\mathbf{V}$ with equation (2) multiplied by $\frac{1}{2}\mathbf{V}\cdot\mathbf{V}$:

$$\frac{\partial}{\partial t}\left(\frac{1}{2}\mathbf{V}\cdot\mathbf{V}h\right)+\nabla\cdot\left[\mathbf{V}\left(\frac{1}{2}\mathbf{V}\cdot\mathbf{V}h\right)\right]+gh\mathbf{V}\cdot\nabla h=0. \tag{4}$$

This equation, together with gh times equation (2) yields the energy equation

$$\frac{\partial}{\partial t}\left[\frac{1}{2}(\mathbf{V}\cdot\mathbf{V}h+gh^2)\right]+\nabla\cdot\left[\mathbf{V}\left(\frac{1}{2}\mathbf{V}\cdot\mathbf{V}h+gh^2\right)\right]=0. \tag{5}$$

The total energy $\frac{1}{2}(\mathbf{V}\cdot\mathbf{V}h+gh^2)$ is seen to be conserved when integrated over the domain with boundary effects neglected.

We now wish to develop difference approximations to these partial differential equations and study their properties. Such approximations are easiest to develop from area integrals of the flux form of the equations. Consider integrals of equations (2) and (3) over some elementary grid area A yet to be defined:

$$\frac{\partial}{\partial t}\int_A h\mathbf{V}dA=-\int_A\nabla\cdot(\mathbf{V}h\mathbf{V})dA-\int_A\nabla g\frac{h^2}{2}dA \tag{6}$$

and

$$\frac{\partial}{\partial t}\int_A hdA=-\int_A\nabla\cdot(h\mathbf{V})dA. \tag{7}$$

The area integrals on the right-hand side can be transformed to line integrals along the boundary S of A:

$$\frac{\partial}{\partial t}\int_A h\mathbf{V}dA=-\oint_S V_n h\mathbf{V}dS-\oint_S g\frac{h^2}{2}\mathbf{n}dS \tag{8}$$

and

$$\frac{\partial}{\partial t}\int_A hdA=-\oint_S V_n h dS \tag{9}$$

where V_n is the velocity component normal to the curve S and $\mathbf{n}$ is the outward unit vector normal to S. The relation used to transform the gradient term holds only in Cartesian coordinates. In spherical coordinates, the pressure gradient term must be handled differently.

3. CONSERVATIVE DIFFERENCE SCHEMES

The difference schemes developed here are all written for a topologically regular grid in the sense that each grid point is surrounded by six triangles. Difference equations expressing the change of a variable at a grid point are written using local polar indexing. The value of some variable ψ at a central point is denoted by ψ_0. The values at surrounding points are then denoted by $\psi_{i,j}=\psi(r_i,\theta_j)$. The r_i is the row radius of the point; $i=1$ for a grid point one triangle from the center, 2 for a point two triangles out, etc. The θ_j is the azimuthal angle, $j=1$ for some reference line, 2 for a point 60° counterclockwise on a topological map of the grid, 3 for a point 120°, etc. See figure 1.

With this notation, a set of difference approximations to equations (8) and (9) conserving mass and momentum is given by

$$A_0\frac{\partial}{\partial t}h_0\mathbf{V}_0+\sum_{i=1}^{6}\delta_i(V_n h\mathbf{V})_{1/2,i}+\sum_{i=1}^{6}g\delta_i\left(\mathbf{n}\frac{h^2}{2}\right)_{1/2,i}=0 \tag{10}$$

and

$$A_0\frac{\partial}{\partial t}h_0+\sum_{i=1}^{6}\delta_i(V_n h)_{1/2,i}=0. \tag{11}$$

A_0 is the area of the hexagon whose sides go through $(1/2, i)$ and are perpendicular to the grid lines, δ_i is the length of the side through $(1/2, i)$, $\mathbf{n}_{1/2,i}$ is the outward unit vector normal to the side, and V_n is the velocity component normal to the side. $(V_n h\mathbf{V})_{1/2,i}$, $(h^2/2)_{1/2,i}$, and $(V_n h)_{1/2,i}$ are to be related to grid-point values from energy considerations.

Let $\overline{\psi}$ denote the finite-difference equivalent of integration of a quantity ψ over the domain, that is,

$$\overline{\psi}=\frac{1}{A_T}\sum A_0\psi_0$$

where the summation is taken over all grid points, and A_T is the total area.

In order for equations (10) and (11) to conserve energy, the following relations must hold

$$\overline{\frac{1}{2}V_0^2\sum_{i=1}^{6}\delta_i(V_n h)_{1/2,i}}=\overline{\sum_{i=1}^{6}\delta_i\mathbf{V}_0\cdot(V_n h\mathbf{V})_{1/2,i}} \tag{12}$$

and

$$\overline{\sum_{i=1}^{6}g\delta_i\mathbf{V}_0\cdot\mathbf{n}_{1/2,i}\left(\frac{h^2}{2}\right)_{1/2,i}}=-\overline{\sum_{i=1}^{6}g\delta_i h_0(V_n h)_{1/2,i}}. \tag{13}$$

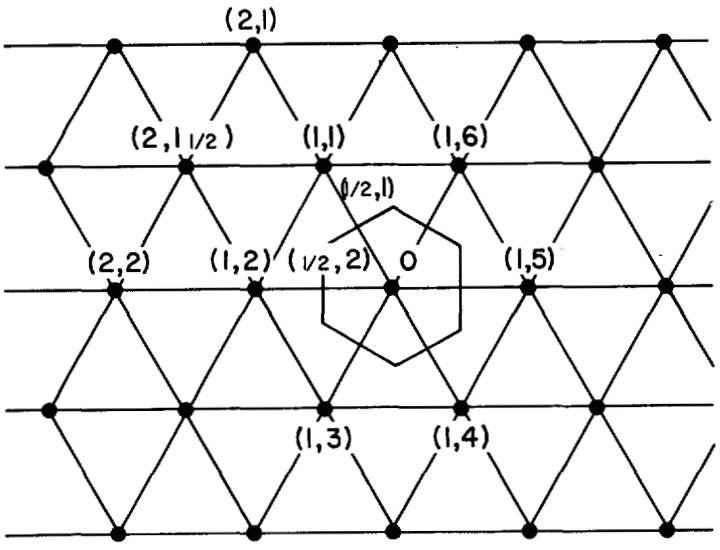

FIGURE 1.—Logical map of a triangular grid.

The first relation (12) insures that the space differences will not produce nonlinear instability; the second (13) provides for consistent conversion between kinetic and potential energy. Equations (12) and (13) are derived from (10) and (11) in the following manner. Split the time derivative of the product $h\mathbf{V}_0$ in (10) into two parts and substitute equation (11). This results in an expression for $h_0\partial\mathbf{V}_0/\partial t$ which is then dotted with $\mathbf{V}_0$. This relation is combined with equation (11) multiplied by $V_0^2/2$ resulting in an expression for $\frac{\partial}{\partial t}\left(h_0\frac{V_0^2}{2}\right)$. This last expression is then combined with equation (11) multiplied by h_0.

If we define

$$(V_n h\mathbf{V})_{1/2,\,i}=\tfrac{1}{2}(\mathbf{V}_0+\mathbf{V}_{1,\,i})(V_n h)_{1/2,\,i}, \tag{14}$$

equation (12) holds because

$$\overline{\sum_{i=1}^{6}\mathbf{V}_0\cdot\mathbf{V}_{1,\,i}(V_n h)_{1/2,\,i}}=0.$$

Differences with the form of (14) have been used by Lorenz (1960), Arakawa (1966), and Bryan (1966).

One possible definition of $(V_n h)_{1/2,\,i}$ is

$$(V_n h)_{1/2,\,i}=\tfrac{1}{2}[h_0\mathbf{V}_0+h_{1,\,i}\mathbf{V}_{1,\,i}]\cdot\mathbf{n}_{1/2,\,i}. \tag{15}$$

The energy conversion relation (13) then holds provided that

$$(h^2)_{1/2,\,i}=h_0 h_{1,\,i}. \tag{16}$$

Expressions (15) and (16) can be verified by substitution into (13) and rearranging and simplifying, noting that $\sum_{i=1}^{6}\delta_i\mathbf{n}_{1/2,\,i}=0$. Substitution of equations (14), (15), and (16) into (10) and (11) results in one energy conservative difference scheme given as:

Scheme I—where

$$\begin{aligned}\frac{\partial}{\partial t}h_0\mathbf{V}_0=&-\frac{1}{4A_0}\sum_{i=1}^{6}\delta_i h_0\mathbf{V}_{1,\,i}(\mathbf{V}_0\cdot\mathbf{n}_{1/2,\,i})\\&-\frac{1}{2A_0}\sum_{i=1}^{6}\delta_i h_{1,\,i}\left[\frac{1}{2}(\mathbf{V}_0+\mathbf{V}_{1,\,i})\right](\mathbf{V}_{1,\,i}\cdot\mathbf{n}_{1/2,\,i})\\&-\frac{gh_0}{2A_0}\sum_{i=1}^{6}\delta_i h_{1,\,i}\mathbf{n}_{1/2,\,i}\end{aligned}$$

and (17)

$$\frac{\partial h_0}{\partial t}=-\frac{1}{2A_0}\sum_{i=1}^{6}\delta_i h_{1,\,i}\mathbf{V}_{1,\,i}\cdot\mathbf{n}_{1/2,\,i}.$$

If applied to a square grid, this scheme is seen to be the same as that used by Grimmer and Shaw (1967) and the same as scheme B of Grammeltvedt (1969).

A second possible definition of $(V_n h)_{1/2,\,i}$ is

$$(V_n h)_{1/2,\,i}=\tfrac{1}{4}(h_0+h_{1,\,i})(\mathbf{V}_0+\mathbf{V}_{1,\,i})\cdot\mathbf{n}_{1/2,\,i}. \tag{18}$$

Relation (13) is now valid if

$$(h^2)_{1/2,\,i}=\tfrac{1}{2}(h_0^2+h_{1,\,i}^2). \tag{19}$$

Substitution of equations (14), (18), and (19) into (10) and (11) results in a second energy conservative scheme given by:

Scheme II—where

$$\begin{aligned}\frac{\partial h_0\mathbf{V}_0}{\partial t}=&-\frac{1}{8A_0}\sum_{i=1}^{6}\delta_i(\mathbf{V}_0+\mathbf{V}_{1,\,i})(h_0+h_{1,\,i})[(\mathbf{V}_0+\mathbf{V}_{1,\,i})\cdot\mathbf{n}_{1/2,\,i}]\\&-\frac{g}{4A_0}\sum_{i=1}^{6}\delta_i h_{1,\,i}^2\mathbf{n}_{1/2,\,i}\end{aligned}$$

and (20)

$$\frac{\partial h_0}{\partial t}=-\frac{1}{4A_0}\sum_{i=1}^{6}\delta_i(h_0+h_{1,\,i})(\mathbf{V}_0+\mathbf{V}_{1,\,i})\cdot\mathbf{n}_{1/2,\,i}.$$

We note that the mass flux of scheme I is similar to the semi-momentum scheme by Shuman (1962) and that of scheme II is similar to his filtered factor form. These two schemes are also similar to those designed by Kurihara and Holloway (1967) for use over a quasi-homogeneous spherical grid.

4. INDIVIDUAL APPROXIMATIONS

Difference approximations are now formulated for the individual terms of the governing equations without regard to energy conservation. First, grid vectors which are useful in writing the approximations are defined.

Let $\mathbf{S}_i$ be the vector from the center point 0 to the surrounding point (1, i) (see fig. 2A). The radial subscript is now dropped, all points considered being in the first row around the center point.

Two adjacent points along with the center point form a triangle with values ψ_0, ψ_i, and ψ_{i+1} of some field ψ at its vertices. If ψ varies linearly over this triangle it can be written, following Winslow (1966), as

$$\psi=\psi_0+\mathbf{S}\cdot\nabla\psi_{i+\frac{1}{2}} \tag{21}$$

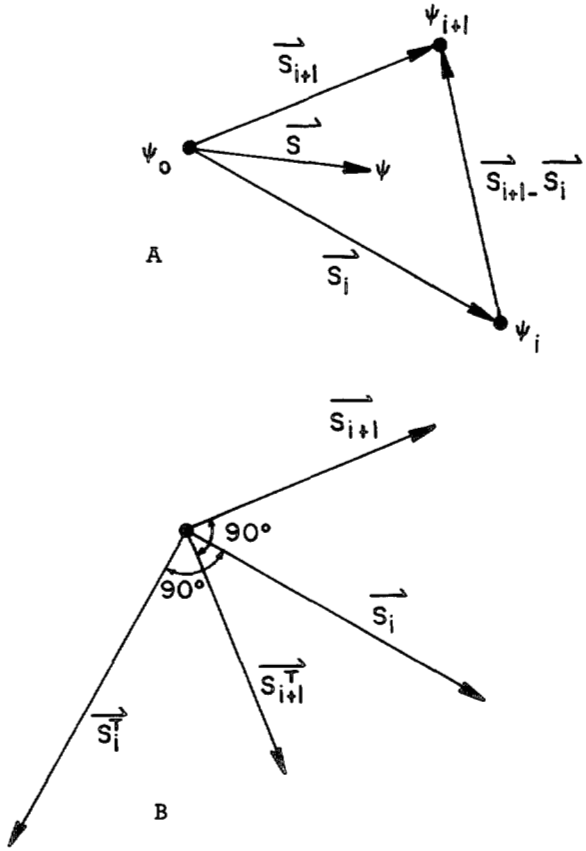

FIGURE 2.—Grid vectors.

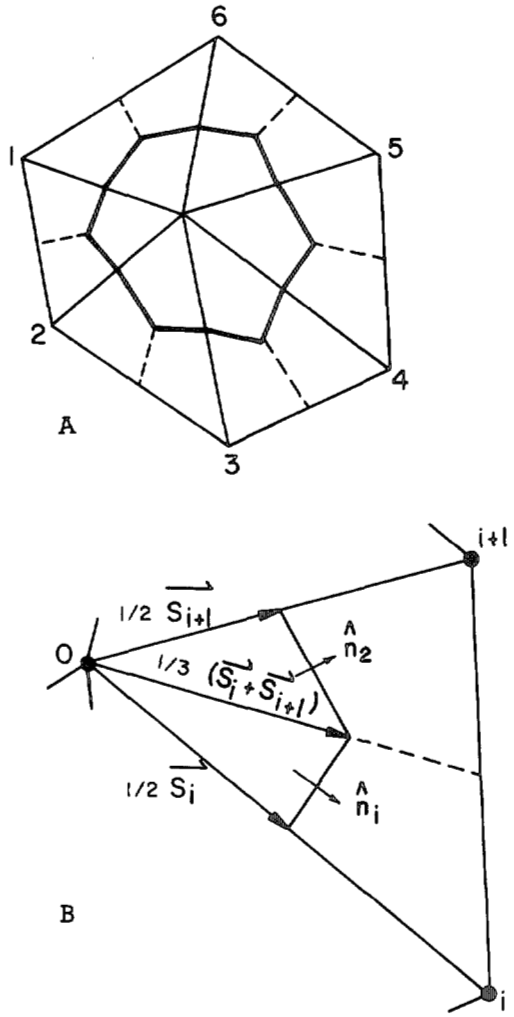

FIGURE 3.—Secondary dodecagonal grid area.

where the gradient is a constant within the triangle and given by

$$\nabla\psi_{i+\frac{1}{2}}=\frac{(\psi_i-\psi_0)\ \mathbf{S}^T_{i+1}-(\psi_{i+1}-\psi_0)\mathbf{S}^T_i}{\mathbf{S}_i\circ\mathbf{S}^T_{i+1}}. \tag{22}$$

$\mathbf{S}$ is the position vector with respect to the center point, and the superscript T denotes a 90° clockwise rotation of a vector (fig. 2B).

A proof of equation (22) is straightforward. Since ψ is assumed to vary linearly in the triangle, it can be written in the following form:

$$\psi=\psi_0+\mathbf{S}\circ[(\psi_i-\psi_0)\mathbf{f}(\mathbf{S}_i,\ \mathbf{S}_{i+1})+(\psi_{i+1}-\psi_0)\mathbf{g}(\mathbf{S}_i,\ \mathbf{S}_{i+1})]$$

where $\mathbf{f}$ and $\mathbf{g}$ are vector functions of $\mathbf{S}_i$ and $\mathbf{S}_{i+1}$. Since $\psi_i=\psi_0+(\psi_i-\psi_0)$, it follows that $\mathbf{S}_i\circ\mathbf{f}=0$ and $\mathbf{S}_i\circ\mathbf{g}=0$. Similarly, $\psi_{i+1}=\psi_0+(\psi_{i+1}-\psi_0)$ implies $\mathbf{S}_{i+1}\circ\mathbf{f}=1$ and $\mathbf{S}_{i+1}\circ\mathbf{g}=1$. Thus, $\mathbf{f}$ and $\mathbf{g}$ have the form $f=C_1\mathbf{S}^T_{i+1}$ and $g=C_2\mathbf{S}^T_i$ where

$$C_1=-C_2=[\mathbf{S}_i\circ\mathbf{S}^T_{i+1}]^{-1}.$$

Define a secondary mesh for the grid to consist of the medians of the grid triangles (fig. 3A). The elementary grid area associated with each grid point is then that of the secondary dodecagon surrounding it.

PRESSURE GRADIENT TERM

Consider the integral of the pressure term over the dodecagonal grid area of figure 3A,

$$I_2=\int_A h\nabla h dA,$$

and assume h varies linearly within each of the six grid triangles. The contribution to the integral from the area $\mathcal{A}$ formed by the intersection of one grid triangle and the dodecagon is

$$I=\int_A(h_0+\mathbf{S}\circ\nabla h)(\nabla h)d\mathcal{A}$$

where the position vector $\mathbf{S}$ is the only variable in the integral. Hence,

$$I=\nabla h\{\mathcal{A}h_0+\nabla h\circ\mathcal{A}\bar{\mathbf{S}}\}.$$

$\bar{\mathbf{S}}$ is the average position vector of the area $\mathcal{A}$.

In the grid triangle defined by $\mathbf{S}_i$ and $\mathbf{S}_{i+1}$, the area $\mathcal{A}$ is that of the two triangles defined by $\frac{1}{2}\mathbf{S}_i$ and $\frac{1}{3}(\mathbf{S}_{i+1}+\mathbf{S}_i)$, and $\frac{1}{3}(\mathbf{S}_{i+1}+\mathbf{S}_i)$ and $\frac{1}{2}\mathbf{S}_{i+1}$ (see fig. 3B). In these two triangles, $\mathcal{A}\bar{\mathbf{S}}$ is

$$\mathcal{A}\bar{\mathbf{S}}=\left(\frac{7}{6}\right)\left(\frac{1}{36}\right)|\mathbf{S}_i\times\mathbf{S}_{i+1}|(\mathbf{S}_i+\mathbf{S}_{i+1}),$$

and $\nabla h\cdot\mathcal{A}\bar{\mathbf{S}}$ is

$$\nabla h_{i+\frac{1}{2}}\cdot\mathcal{A}\bar{\mathbf{S}}=\left(\frac{7}{6}\right)\left(\frac{1}{36}\right)|\mathbf{S}_i\times\mathbf{S}_{i+1}|[(h_i-h_0)+(h_{i+1}-h_0)].$$

Thus,

$$I_2=\sum_{i=1}^{6}\nabla h_{i+\frac{1}{2}}\left\{\mathcal{A}_{i+\frac{1}{2}}h_0+\nabla h_{i+\frac{1}{2}}\cdot\mathcal{A}\bar{\mathbf{S}}\right\}$$

with the above values substituted.

Similarly, other approximations to the pressure term can be defined. Consider the integral

$$I_3=\int_A\nabla\frac{h^2}{2}\,dA$$

and let h^2 vary linearly over the grid triangles. The integral then becomes

$$I_3=\frac{1}{2}\sum_{i=1}^{6}\mathcal{A}_{i+\frac{1}{2}}\nabla h^2_{i+\frac{1}{2}}$$

where the expression for the gradient is given by equation (22).

Another approximation can be formulated from

$$I_4=\oint\mathbf{n}\frac{h^2}{2}\,dS$$

where h^2 is assumed to vary linearly over grid triangles. In this case the line integral becomes simply the trapezoidal rule with values at the vertices of the dodecagon. The integral I_4 can be evaluated other ways, such as by assuming h varies linearly over grid triangles. The line integral does not reduce to the trapezoidal rule in this case.

MASS FLUX

Difference approximations for the mass flux term, right-hand side of equation (23), are now considered:

$$\frac{\partial h}{\partial t}=-\frac{1}{A}\oint_S(\mathbf{V}h)\cdot\mathbf{n}\,dS. \tag{23}$$

Let $\mathbf{V}h$ vary linearly within grid triangles. The two outward normals along the two sides of the dodecagon (fig. 3B) within the grid triangle defined by $\mathbf{S}_i$ and $\mathbf{S}_{i+1}$ are given by

$$\mathbf{n}_1=\frac{\mathbf{S}^T_{i+1}-\frac{1}{2}\mathbf{S}^T_i}{\left|\mathbf{S}^T_{i+1}-\frac{1}{2}\mathbf{S}^T_i\right|}$$

and

$$\mathbf{n}_2=\frac{\frac{1}{2}\mathbf{S}^T_{i+1}-\mathbf{S}^T_i}{\left|\frac{1}{2}\mathbf{S}^T_{i+1}-\mathbf{S}^T_i\right|}.$$

Substituting these expressions for $\mathbf{n}_1$ and $\mathbf{n}_2$, plus equations (21) and (22) for $\mathbf{V}h$ into equation (23) along with some manipulation, leads to the difference equation

$$\frac{\partial h_0}{\partial t}=-\frac{1}{6A_0}\sum_{i=1}^{6}\mathbf{V}_ih_i\cdot(\mathbf{S}^T_{i+1}-\mathbf{S}^T_{i-1}). \tag{24}$$

Another approximation can be derived by assuming both h and $\mathbf{V}$ vary linearly over grid triangles and approximating the line integral in equation (23) with the trapezoidal rule between vertices of the dodecagon. This approximation becomes

$$\frac{\partial h_0}{\partial t}=-\frac{5}{72}\frac{1}{A_0}\sum_{i=1}^{6}[h_i\mathbf{V}_0+h_0\mathbf{V}_i+h_i\mathbf{V}_i]\cdot(\mathbf{S}^T_{i+1}-\mathbf{S}^T_{i-1})$$
$$+\frac{1}{36}\frac{1}{A_0}\sum_{i=1}^{6}(h_{i+1}\mathbf{V}_i+h_i\mathbf{V}_{i+1})\cdot(\mathbf{S}^T_{i+1}-\mathbf{S}^T_i). \tag{25}$$

Other approximations can be found by making assumptions similar to those made in approximating the pressure gradient term.

MOMENTUM FLUX

Approximations for the momentum flux term on the right-hand side of the following equation

$$\frac{\partial h\mathbf{V}}{\partial t}=-\frac{1}{A}\oint_S(\mathbf{V}h)\mathbf{V}\cdot\mathbf{n}dS \tag{26}$$

can be obtained using the same methods as the mass advection. For example, if $\mathbf{V}h\mathbf{V}$ is assumed to vary linearly within grid triangles, the resulting expression for equation (26) becomes

$$\frac{\partial h\mathbf{V}}{\partial t}=-\frac{1}{6A}\sum_{i=1}^{6}\mathbf{V}_ih_i\mathbf{V}_i\cdot(\mathbf{S}^T_{i+1}-\mathbf{S}^T_{i-1}). \tag{27}$$

By making approximations similar to those made for the mass flux, other difference schemes can be obtained.

5. HOMOGENEOUS GRID

We now consider the form these schemes take when applied to an equilateral triangular (homogeneous) grid and determine the truncation error of such approximations. Consider Cartesian coordinates (x, y) with unit vectors $(\mathbf{i}, \mathbf{j})$. Let δ be the constant distance between grid

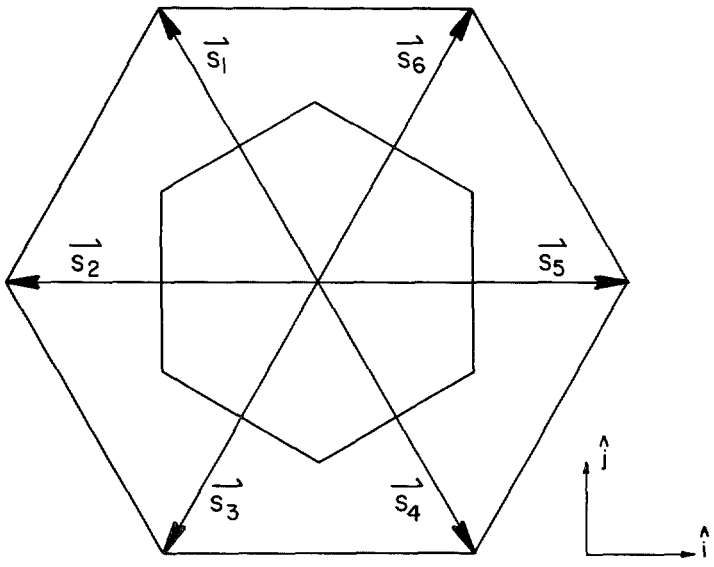

FIGURE 4.—Homogeneous grid vectors.

points, and define the grid vectors $\mathbf{S}_i$ by

$$\mathbf{S}_1=-\frac{1}{2}\delta\mathbf{i}+\frac{\sqrt{3}}{2}\delta\mathbf{j},$$

$$\mathbf{S}_2=-\delta\mathbf{i},$$

$$\mathbf{S}_3=-\frac{1}{2}\delta\mathbf{i}-\frac{\sqrt{3}}{2}\delta\mathbf{j},$$

$$\mathbf{S}_4=\frac{1}{2}\delta\mathbf{i}-\frac{\sqrt{3}}{2}\delta\mathbf{j},$$

$$\mathbf{S}_5=\delta\mathbf{i}, \text{ and}$$

$$\mathbf{S}_6=\frac{1}{2}\delta\mathbf{i}+\frac{\sqrt{3}}{2}\delta\mathbf{j}.$$

See figure 4.

Consider first the pressure term on the right-hand side of the equation,

$$\frac{\partial}{\partial t}(h\mathbf{V})_0=-\frac{1}{A}\int_A gh\nabla h\,dA,$$

or an equivalent form. We denote discrete approximations to the right-hand side as P_j.

Since

$$\sum_{i=1}^{6}\mathbf{S}_i=0$$

and

$$\mathbf{n}_{1/2,i}=\mathbf{S}_i/|\mathbf{S}_i|,$$

the pressure gradient term of scheme I can be written as

$$P_1=-g\sum_{i=1}^{6}h_0\frac{h_i-h_0}{3\delta^2}\mathbf{S}_i.$$

Noting that

$$\mathbf{S}^T_{i+1}-\mathbf{S}^T_{i-1}=\sqrt{3}\mathbf{S}_i$$

and

$$\mathbf{S}^T_{i+1}-\mathbf{S}^T_i=\frac{\sqrt{3}}{3}(\mathbf{S}_i+\mathbf{S}_{i+1}),$$

the scheme corresponding to the intergral I_2 is

$$P_2=-g\sum_{i=1}^{6}\left[\frac{73}{108}h_0+\frac{21}{108}h_1+\frac{7}{108}h_{i+1}+\frac{7}{108}h_{i-1}\right]\frac{h_i-h_0}{3\delta^2}\mathbf{S}_i.$$

The pressure gradient term of scheme II and the scheme corresponding to I_3 both become

$$P_3=-g\sum_{i=1}^{6}\left(\frac{1}{2}h_0+\frac{1}{2}h_i\right)\frac{h_i-h_0}{3\delta^2}\mathbf{S}_i,$$

and that corresponding to I_4 becomes

$$P_4=-g\sum_{i=1}^{6}\frac{1}{6}[(h^2_{i-1}+h^2_i+h^2_0)+(h^2_i+h^2_{i+1}+h^2_0)]\frac{\mathbf{S}_i}{3\delta^2},$$

which can be shown to be the same as P_3.

The mass flux scheme from the right-hand side of equation (24) when applied to the homogeneous grid becomes

$$Q_1=-\frac{1}{3\delta^2}\sum_{i=1}^{6}h_i\mathbf{V}_i\cdot\mathbf{S}_i.$$

The mass flux term of scheme I also reduces to this expression. The mass flux of scheme II becomes

$$Q_2=-\frac{1}{3\delta^2}\sum_{i=1}^{6}\frac{1}{2}[h_0\mathbf{V}_i+h_i\mathbf{V}_0+h_i\mathbf{V}_i]\cdot\mathbf{S}_i,$$

and the right-hand side of equation (25) reduces to

$$Q_3=\frac{5}{6}Q_2-\frac{1}{3\delta^2}\sum_{i=1}^{6}\frac{1}{18}[(h_{i+1}+h_{i-1})\mathbf{V}_i+h_i(\mathbf{V}_{i+1}+\mathbf{V}_{i-1})]\cdot\mathbf{S}_i.$$

The momentum flux on the right-hand side of equation (27) when applied to this grid becomes

$$M_1=-\frac{1}{3\delta^2}\sum_{i=1}^{6}(\mathbf{V}_ih_i\mathbf{V}_i)\cdot\mathbf{S}_i,$$

while the momentum flux of scheme I reduces to

$$M_2=-\frac{1}{3\delta^2}\sum_{i=1}^{6}\frac{1}{2}h_0\mathbf{V}_i(\mathbf{V}_0\cdot\mathbf{S}_i)$$
$$-\frac{1}{3\delta^2}\sum_{i=1}^{6}h_i\left[\frac{1}{2}(\mathbf{V}_0+\mathbf{V}_i)\right](\mathbf{V}_i\cdot\mathbf{S}_i).$$

The momentum flux of scheme II becomes

$$M_3=-\frac{1}{3\delta^2}\sum_{i=1}^{6}\frac{1}{4}(\mathbf{V}_0+\mathbf{V}_i)(h_0+h_i)(\mathbf{V}_0+\mathbf{V}_i)\cdot\mathbf{S}_i.$$

6. TRUNCATION ERROR

In section 4, energy conservative schemes are developed. These energy conservation conditions do not, however, require local accuracy. In section 5, schemes are developed using methods which immediately lead to consistent approximations. Again, however, it does not necessarily follow that the schemes are locally accurate. Therefore, it is useful to examine the truncation errors of these schemes.

The truncation error of the approximations is determined by substituting Taylor's series expansions about the center point into the difference approximations and com-

paring the result with the continuous term. Let

$$h_{i,l}=h_0+\sum_{j=1}^{\infty}\frac{1}{j!}[(\mathbf{S}_{i,l}\cdot\nabla)^j h]_0$$

and

$$\mathbf{V}_{i,l}=\mathbf{V}_0+\sum_{j=1}^{\infty}\frac{1}{j!}[(\mathbf{S}_{i,l}\cdot\nabla)^j\mathbf{V}]_0. \tag{28}$$

These expressions are substituted into schemes P_k, Q_k, and M_k, and like powers of δ are combined. Some relations prove useful in simplifying these combinations; these are listed in the appendix. All are easily verified by expansion into Cartesian components.

Using these relations, the Taylor's series expansions of schemes P_k simplify to

$$P_1=-gh_0\nabla h_0-\delta^2\frac{g}{8}h_0\nabla(\nabla^2 h_0)+0(\delta^4),$$

$$P_2=-gh_0\nabla h_0-\delta^2\frac{g}{144}[7\nabla(\nabla\cdot h\nabla h)+11h\nabla(\nabla^2 h)+7\nabla^2 h\nabla h]_0+0(\delta^4),$$

and

$$P_3=P_4=-gh_0\nabla h_0-\delta^2\frac{g}{8}\nabla(\nabla\cdot h\nabla h)_0+0(\delta^4).$$

These schemes are all seen to be second order.

The Taylor's series expansions of the mass advection schemes become

$$Q_1=-\nabla\cdot(h\mathbf{V})_0-\delta^2\frac{1}{8}\{\mathbf{V}\cdot\nabla(\nabla^2 h)+h\nabla^2(\nabla\cdot\mathbf{V})+2\nabla^2 h\nabla\cdot\mathbf{V}+2\nabla h\cdot\nabla^2\mathbf{V}+4\nabla\cdot[(\nabla h\cdot\nabla)\mathbf{V}]\}_0+0(\delta^4),$$

$$Q_2=-\nabla\cdot(h\mathbf{V})_0-\delta^2\frac{1}{8}\{\mathbf{V}\cdot\nabla(\nabla^2 h)+h\nabla^2(\nabla\cdot\mathbf{V})+\nabla^2 h\nabla\cdot\mathbf{V}+\nabla h\cdot\nabla^2\mathbf{V}+2\nabla\cdot[(\nabla h\cdot\nabla)\mathbf{V}]\}_0+0(\delta^4),$$

and

$$Q_3=-\nabla\cdot(h\mathbf{V})_0-\delta^2\frac{1}{8}\left\{\mathbf{V}_0\cdot\nabla(\nabla^2 h)+h\nabla^2(\nabla\cdot\mathbf{V})+\frac{7}{9}\nabla^2 h\nabla\cdot\mathbf{V}+\frac{7}{9}\nabla h\cdot\nabla^2\mathbf{V}+\frac{5}{3}\nabla\cdot[(\nabla h\cdot\nabla)\mathbf{V}]\right\}_0+0(\delta^4).$$

All of these schemes are seen to be second order.

The expansions of the momentum advection terms are of the form

$$M_k=-\nabla\cdot(\mathbf{V}h\mathbf{V})_0+\delta^2\mathbf{F}_k(h_0,\mathbf{V}_0)+0(\delta^4).$$

The expressions $\mathbf{F}_k$ $(h_0,\ \mathbf{V}_0)$ are rather long and complicated and are not given here. These schemes are also seen to be second order.

7. FOURTH-ORDER SCHEMES

Straightforward extrapolation techniques can be applied to the second-order schemes derived above to obtain fourth-order schemes. For example, consider the pressure term from the conservative scheme (17)

$$P_1=-g\sum_{i=1}^{6}h_0\frac{h_{1,i}-h_0}{3\delta^2}\mathbf{S}_i$$

where we have resumed the use of the radial subscript. If this scheme is applied to the triangles formed by the points $h_{2,i}$ with h_0, the approximation is the same as P_1 except δ is replaced by 2δ and $\mathbf{S}_i$ by $2\mathbf{S}_i$. Hence, we have a scheme

$$P_1'=-\frac{g}{2}\sum_{i=1}^{6}h_0\frac{h_{2,i}-h_0}{3\delta^2}\mathbf{S}_i$$

with a Taylor's series expansion

$$P_1'=-gh_0\nabla h_0-\delta^2\frac{g}{2}h_0\nabla(\nabla^2 h_0)+0(\delta^4).$$

These two schemes can then be combined in the form $P_1^*=AP_1+BP_1'$, where A and B are found by requiring that the coefficient of δ^2 in the Taylor expansion of P_1^* be zero and the coefficient of $-gh\nabla h$ be 1. The solution is $A=4/3$, $B=-1/3$, and the fourth-order approximation is

$$P_1^*=-g\sum_{i=1}^{6}h_0\left(\frac{4}{3}h_{1,i}-\frac{1}{6}h_{2,i}-\frac{7}{6}h_0\right)\frac{\mathbf{S}_i}{3\delta^2}.$$

This same extrapolation can be applied to all the terms of the energy conservative scheme (17). Such a fourth-order scheme is also energy conservative since each of its two parts are.

Another possibility is to use the points $\left(2,\ i+\frac{1}{2}\right)$ rather than $(2,\ i)$. These are closer to the center point than the points $(2,\ i)$, and are not lined up with the points $(1,\ i)$; and hence they might make a better approximation. In this case δ in the truncation error is replaced by $\sqrt{3}\ \delta$, and the combination coefficients become $A=3/2$ and $B=-1/2$. The fourth-order energy conservative scheme corresponding to (17) is given by:

Scheme III—where

$$\frac{\partial h_0\mathbf{V}_0}{\partial t}=-\frac{1}{4\delta}\sum_{i=1}^{6}\{h_0\mathbf{V}_{1,i}(\mathbf{V}_0\cdot\mathbf{n}_{1/2,i})+h_{1,i}(\mathbf{V}_0+\mathbf{V}_{1,i})\times(\mathbf{V}_{1,i}\cdot\mathbf{n}_{1/2,i})+2gh_{1,i}\mathbf{n}_{1/2,i}\}+\frac{1}{12\sqrt{3}\delta}\sum_{i=1}^{6}\{h_0\mathbf{V}_{2,i+\frac{1}{2}}(\mathbf{V}_0\cdot\mathbf{n}_{1,i+\frac{1}{2}})+h_{2,i+\frac{1}{2}}(\mathbf{V}_0+\mathbf{V}_{2,i+\frac{1}{2}})(\mathbf{V}_{2,i+\frac{1}{2}}\cdot\mathbf{n}_{1,i+\frac{1}{2}})+2gh_{2,i+\frac{1}{2}}\mathbf{n}_{1,i+\frac{1}{2}}\} \tag{29}$$

and

$$\frac{\partial h_0}{\partial t}=-\frac{1}{2\delta}\sum_{i=1}^{6}h_{1,i}\mathbf{V}_{1,i}\cdot\mathbf{n}_{1/2,i}+\frac{1}{6\sqrt{3}\delta}\sum_{i=1}^{6}h_{2,i+\frac{1}{2}}\mathbf{V}_{2,i+\frac{1}{2}}\cdot\mathbf{n}_{1,i+\frac{1}{2}}.$$

8. BOUNDARY CONDITIONS

We now consider the lateral boundary condition for an inviscid fluid when the boundary is a straight line coinciding with the sides of grid triangles. The boundary condition for the continuous equations is that there should be no normal flow across the boundary.

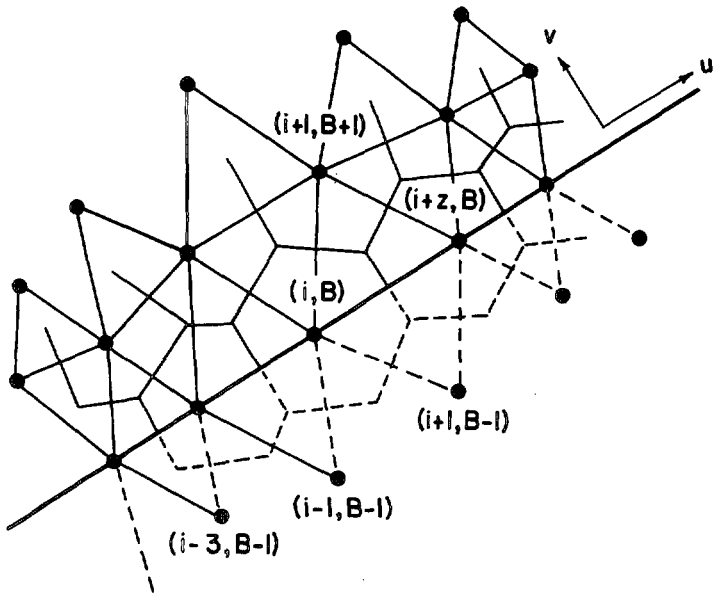

FIGURE 5.—Boundary grid points.

Denote the tangential and normal components of the velocity $\mathbf{V}$ by u and v, respectively. Define a row of grid points outside the boundary to be the mirror image of the first row of points inside the boundary (fig. 5). Define a subscript (i, j) such that $j = B$ if the point is on the boundary, $j = B+1$ ($j = B-1$) if the point is in the first row inside (outside) the boundary, and i is an index along the boundary from some reference point. These subscripts, applied to the components u, v, and h should not be confused with the radial, azimuthal subscripts applied to the vectors.

With this notation, the discrete boundary condition becomes $v_{i,B} = 0$. If we define

$$h_{i,B-1}=h_{i,B+1},$$

$$u_{i,B-1}=u_{i,B+1},$$

and

$$v_{i,B-1}=-v_{i,B+1}, \tag{30}$$

difference equations of the form (10), (11) applied to the boundary points result in

$$\frac{\partial h_0 v_0}{\partial t}=0$$

if $(V_n h\mathbf{V})_{1/2,i}$, $(h^2/2)_{1/2,i}$, and $(V_n h)_{1/2,i}$ are evaluated using only values at (0) and $(1,i)$. Thus if $v_{i,B}$ is initially zero, it will remain zero. It is also seen that the area-weighted averages of mass and momentum over the domain are conserved when the boundary values are weighted by that part of their grid area inside the domain and that the energy conserving schemes (17) and (20) continue to conserve energy using these boundary conditions.

These boundary conditions hold only for pure gravity wave motions associated with equations (1) and (2). When the Coriolis term is included in the governing equations, the boundary conditions are no longer exact. Since the initial conditions for the test cases presented here are such that there is very little motion near the boundary and since the integrations are carried out for a relatively short time, little trouble is expected in using these boundary conditions.

9. NUMERICAL INTEGRATIONS

Ten-day integrations were performed using several of the schemes developed here over an equilateral triangular grid on a beta plane. The Coriolis term was differenced by simply using the value of the velocity at the central point, thus the schemes remain energy conservative. When conservative scheme (17) is applied to the right triangles corresponding to a square net of points, it is seen to be the same as scheme B of Grammeltvedt (1969). For this reason it was decided to use the same initial conditions as he used. A direct comparison between four- and six-point differences is then possible. His initial condition I is given by

$$h(x,y)=H_0+H_1\tanh\frac{9(y_0-y)}{2D}+H_2\,\mathrm{sech}^2\frac{9(y_0-y)}{D}\sin\left(\frac{2\pi x}{L}\right)$$

where x is the eastward coordinate, y the northward, y_0 the center of the channel, L the length of the channel, and D the width. The initial velocity fields are assumed to be geostrophic.

The following values are adopted for the constants:

$H_0=2000$ m,	$L=6000$ km,
$H_1=220$ m,	$D=\sqrt{3}\times 2600$ km,
$H_2=133$ m,	$f=10^{-4}$ sec^{-1},
$g=10$ m sec^{-2},	$\beta=10^{-11}$ sec^{-1} m^{-1}.

The length δ of the sides of the equilateral triangles forming the grid was taken to be either 100, 200, 231, or 270 km. The north-south boundary conditions are equation (30) with the additional requirement that v on the boundary be held at zero. These are equivalent to those used by Grammeltvedt (1969). The east-west boundary conditions are cyclic. A 10-min time step is used when δ equals 200 km or more, and a 5-min step when δ equals 100 km. Figure 6 shows the initial height field.

The height fields after 5 days for eight different cases are shown in figure 7. The top left is obtained by Grammeltvedt's square scheme F using a fine mesh with δ equal to 100 km, and the top right is due to scheme I also using a fine mesh with δ equal to 100 km. Since these two solutions are almost identical, we can assume they represent the correct solution. The scheme used for the left of the second row is Grammeltvedt's square scheme B with a coarser resolution of δ equal to 200 km, and the scheme used for the right is triangular scheme I with the same value of δ. The triangular scheme is seen to

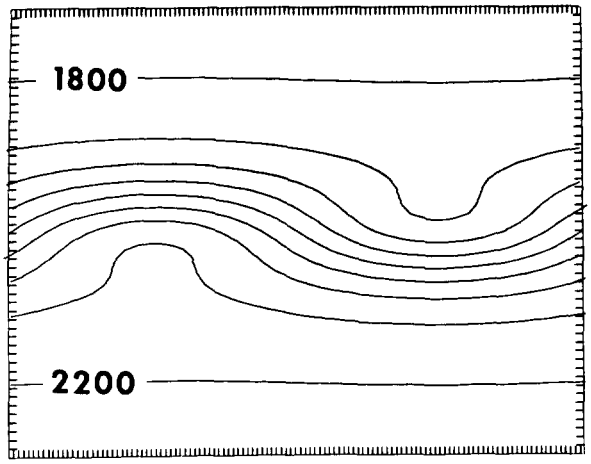

FIGURE 6.—Initial height field; heights in meters; contour interval, 500 m.

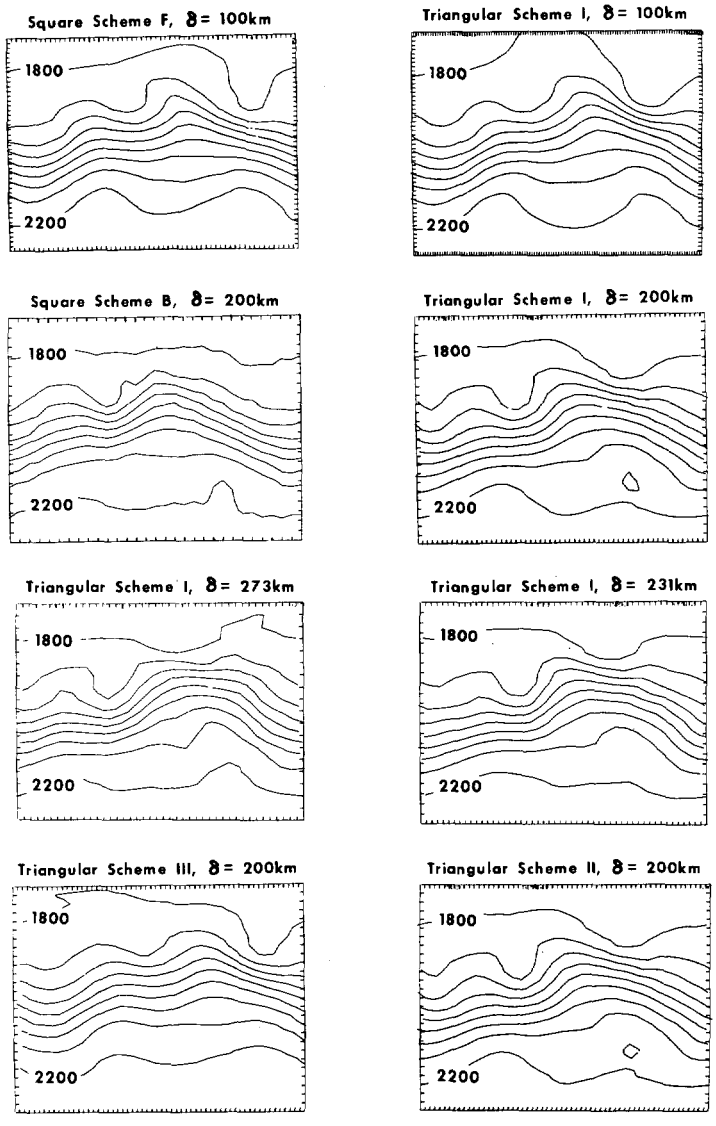

FIGURE 7.—Height fields after 5 days; heights in meters; contour interval, 500 m; see section 9 for explanation.

be better than the square scheme. Both the phase error and amplitude errors are less for the former.

From these results it is not clear whether or not the triangular scheme is better because it has slightly better resolution in the y-direction. Since the base of a grid triangle is the same length as a side of the square grid, the height of the triangles is less than that of the squares, resulting in more grid points in the y-direction in the triangular grid than in the square grid. To determine the effect of this difference in resolution, the triangular scheme was integrated over a grid with the height of the triangles equal to 200 km, or δ approximately equal to 231 km. The results are presented on the right side of the third row of figure 7. The solution hardly differs from the case in which δ equals 200 km and is again better than the square scheme. Scheme I was integrated with an even coarser resolution of δ approximately 273 km. The result is on the left of the third row of figure 7. This solution is seen to be at least as good as that for the square scheme B. Thus, we conclude that the slightly better resolution in the y-direction of the triangular schemes is not the main reason for their better solutions.

The bottom right of figure 7 is obtained from triangular scheme II. The field is seen to be almost identical to that of scheme I. The lower left is due to fourth-order triangular scheme III. The phase and amplitude have very little error when compared with the fine resolution results. If the fourth-order scheme III is compared with Grammeltvedt's fourth-order square scheme J (his fig. 8), the triangular scheme is again seen to be better.

Figure 8 shows the height fields after 10 days. Now the solutions of the two fine resolution schemes are beginning to diverge. The main feature is wave number 2. The triangular schemes all exhibit this wave number 2 much better than the square scheme B. The phase error of the fourth-order scheme is less than the second-order schemes and is also less than the phase error for Grammelvedt's fourth-order square scheme J as seen in his figure 8. These schemes can also be compared with Shuman's scheme (Grammeltvedt's fig. 9) which is seen to have a much greater phase truncation error.

10. CONCLUSIONS

The schemes compared here indicate that, for numerical modeling of atmospherelike fluid flow, homogeneous triangular difference approximations provide better solutions than homogeneous square approximations with similar resolution and the same order of truncation error.

It should be pointed out that the triangular schemes require slightly more computer time than the square schemes if both grids contain the same number of grid points. This follows from the fact that the number of computations required to calculate the time derivatives depends on the number of grid points times the number of

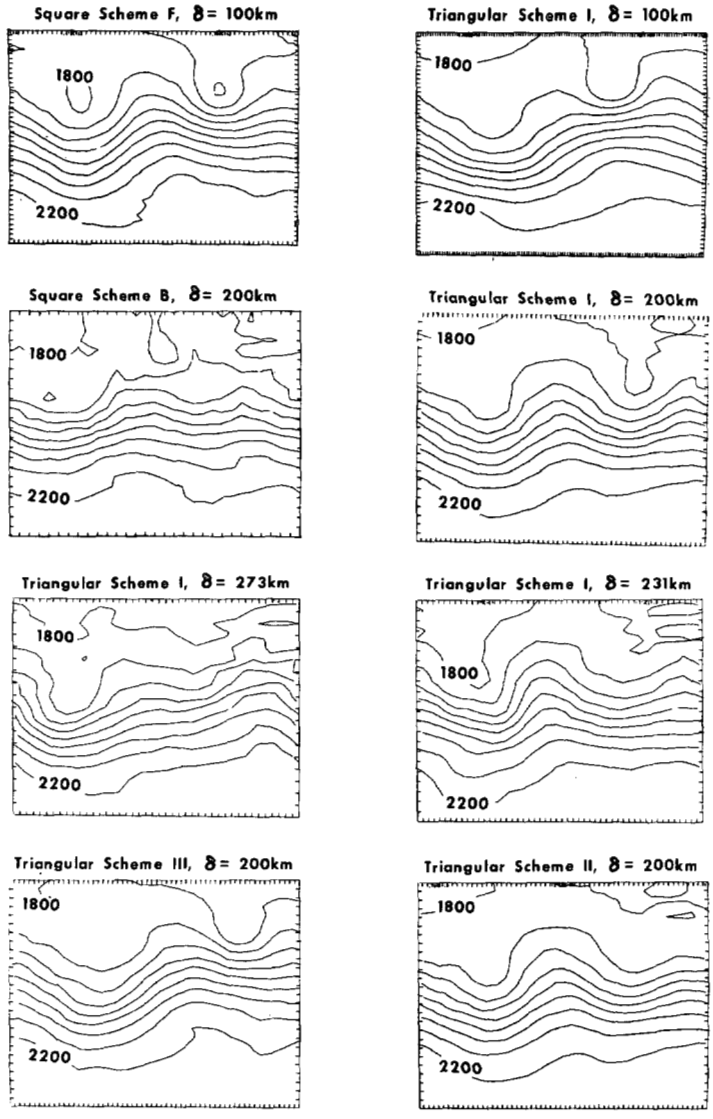

FIGURE 8.—Height fields after 10 days; heights in meters; contour interval, 500 m; see section 9 for explanation.

surrounding points. The actual computer times needed to integrate, say, scheme I and scheme B for the same grid interval were almost the same. Since a triangular grid integrated over a coarser grid produces as good a result as a square scheme over a less coarse grid, the triangular schemes actually produce a saving of computer time for the same quality of solution.

APPENDIX

RELATIONS USED TO SIMPLIFY TRUNCATION ERROR EXPRESSIONS (SEE SECTION 6)

Relation 1—

$$\frac{1}{3\delta^2}\sum_{i=1}^{6}(\mathbf{S}_i\cdot\nabla)^k h_0\mathbf{S}_i=0 \text{ for even } k,$$
$$=\nabla h_0 \text{ for } k=1,$$
$$=\frac{3}{4}\delta^2\nabla(\nabla^2 h_0) \text{ for } k=3,$$
$$\leq 0(\delta^{k-1}) \text{ for odd } k>3,$$

and

$$\frac{1}{3\delta^2}\sum_{i=1}^{6}(\mathbf{S}_i\cdot\nabla)^k\mathbf{V}_0\cdot\mathbf{S}_i=0 \text{ for even } k,$$
$$=\nabla\cdot\mathbf{V}_0 \text{ for } k=1,$$
$$=\frac{3}{4}\delta^2\nabla\cdot(\nabla^2\mathbf{V}) \text{ for } k=3,$$
$$\leq 0(\delta^{k-1}) \text{ for odd } k>3.$$

Relation 2—

$$\sum_{\substack{j+k=l\\ j,k\neq 0}}\frac{1}{3\delta^2}\sum_{i=1}^{6}[(\mathbf{S}_i\cdot\nabla)^j h_0][(\mathbf{S}_i\cdot\nabla)^k h_0]\mathbf{S}_i=0 \text{ for } l \text{ even},$$
$$=\frac{1}{2}\delta^2\{\nabla^2 h\nabla h+\nabla[(\nabla h)^2]\}_0 \text{ for } l=3,$$
$$\leq 0(\delta^{l-1}) \text{ for odd } l>3,$$
$$\sum_{\substack{j+k=l\\ j,k\neq 0}}\frac{1}{3\delta^2}\sum_{i=1}^{6}[(\mathbf{S}_i\cdot\nabla)^j h_0][(\mathbf{S}_i\cdot\nabla)^k\mathbf{V}_0]\cdot\mathbf{S}_i=0 \text{ for } l \text{ even}$$
$$=\frac{1}{2}\delta^2\{\nabla^2 h\nabla\cdot\mathbf{V}+\nabla h\cdot\nabla^2\mathbf{V}+2\nabla\cdot[(\nabla h\cdot\nabla)\mathbf{V}]\} \text{ for } l=3,$$
$$\leq 0(\delta^{l-1}) \text{ for odd } l>3,$$

and

$$\sum_{\substack{j+k=l\\ j,k\neq 0}}\frac{1}{3\delta^2}\sum_{i=1}^{6}[(\mathbf{S}_i\cdot\nabla)^j\mathbf{V}_0][(\mathbf{S}_i\cdot\nabla)^k h_0]\mathbf{V}_0\cdot\mathbf{S}_i=0 \text{ for } l \text{ even},$$
$$=\frac{1}{4}\delta^2\{\nabla^2\mathbf{V}(\mathbf{V}\cdot\nabla h)+\nabla^2 h(\mathbf{V}\cdot\nabla\mathbf{V})+2\mathbf{V}\cdot\nabla(\mathbf{V}h\cdot\nabla\mathbf{V})\}_0 \text{ for } l=3,$$
$$\leq 0(\delta^{l-1}) \text{ for odd } l>3.$$

Relation 3—

$$\frac{1}{3\delta^2}\sum_{i=1}^{6}[(\mathbf{S}_{i+1}\cdot\nabla)^j h_0+(\mathbf{S}_{i-1}\cdot\nabla)^j h_0]\mathbf{S}_i=0 \text{ for } j \text{ even},$$
$$=\nabla h_0 \text{ for } j=1,$$
$$=\frac{3}{4}\delta^2\nabla(\nabla^2 h_0) \text{ for } j=3,$$
$$\leq 0(\delta^{j-1}) \text{ for odd } j>3,$$

and

$$\frac{1}{3\delta^2}\sum_{i=1}^{6}[(\mathbf{S}_{i+1}\cdot\nabla)^j+(\mathbf{S}_{i-1}\cdot\nabla)^j]\mathbf{V}_0\cdot\mathbf{S}_i=0 \text{ for } j \text{ even},$$
$$=\nabla\cdot\mathbf{V}_0 \text{ for } j=1,$$
$$=\frac{3}{4}\delta^2\nabla\cdot(\nabla^2\mathbf{V}_0) \text{ for } j=3,$$
$$\leq 0(\delta^{j-1}) \text{ for odd } j>3.$$

Relation 4—

$$\sum_{\substack{j+k=l \\ j,\,k\neq 0}} \frac{1}{3\delta^2} \sum_{i=1}^{6} [\mathbf{S}_{i+1}\cdot\nabla)^j h_0 + (\mathbf{S}_{i-1}\cdot\nabla)^j h_0]\,(\mathbf{S}_i\cdot\nabla)^k h_0 \mathbf{S}_i$$

$$= 0 \text{ for } l \text{ even},$$

$$= \frac{3}{2}\delta^2 \nabla^2 h_0 \nabla h_0 \text{ for } l=3,$$

$$\leq 0(\delta^{l-1}) \text{ for odd } l>3$$

and

$$\sum_{\substack{j+k=l \\ j,\,k\neq 0}} \frac{1}{3\delta^2} \Bigg\{ \sum_{i=1}^{6} [(\mathbf{S}_i\cdot\nabla)^j h_0]\,[(\mathbf{S}_{i+1}\cdot\nabla)^k + (\mathbf{S}_{i-1}\cdot\nabla)^k]\mathbf{V}_0\cdot\mathbf{S}_i$$

$$+ \sum_{i=1}^{6} [\mathbf{S}_{i+1}\cdot\nabla)^j h_0 + (\mathbf{S}_{i-1}\cdot\nabla)^j h_0](\mathbf{S}_i\cdot\nabla)^k \mathbf{V}_0\cdot\mathbf{S}_i \Bigg\}$$

$$= 0 \text{ for } l \text{ even},$$

$$= \frac{3}{2}\delta^2[\nabla^2\mathbf{V}\cdot\nabla h + \nabla^2 h \nabla\cdot\mathbf{V}]_0 \text{ for } l=3,$$

$$\leq 0(\delta^{l-1}) \text{ for odd } l>3.$$

Relation 5—

$$\sum_{\substack{j+k+l=m \\ j,\,k,\,l\neq 0}} \frac{1}{3\delta^2} \sum_{i=1}^{6} [(\mathbf{S}_i\cdot\nabla)^j \mathbf{V}_0][(\mathbf{S}_i\cdot\nabla)^k h_0](\mathbf{S}_i\cdot\nabla)^l \mathbf{V}_0\cdot\mathbf{S}_i$$

$$= 0 \text{ for } m \text{ even},$$

$$= \tfrac{1}{4}\{(\nabla\cdot\mathbf{V})(\nabla h\cdot\nabla\mathbf{V}) + (\nabla h\cdot\nabla\mathbf{V})\cdot\nabla\mathbf{V}$$

$$+ \nabla(\mathbf{V}\cdot\nabla h)\cdot\nabla h - [(\mathbf{V}\cdot\nabla)\nabla h]\cdot\nabla\mathbf{V}\}_0$$

$$\text{for } m=3,$$

$$\leq 0(\delta^{m-1}) \text{ for odd } m>3.$$

ACKNOWLEDGMENTS

The author would like to thank Drs. Lorenz of MIT and Kasahara of NCAR for their encouragement during this work and for reading the manuscript carefully. Thanks are also due Drs. Arakawa of UCLA and Grammeltvedt and Washington of NCAR for discussions about difference schemes, and to Dr. Grammeltvedt for permission to use his figures showing results of the square difference schemes.

The formulation of the difference schemes was performed at MIT under Weather Bureau contract number E22-3-68(N). The numerical experiments were performed when the author was a student visitor in the Dynamics Group at NCAR.

REFERENCES

Arakawa, A., "Computational Design for Long-Term Numerical Integration of the Equations of Fluid Motion: I. Two-Dimensional Incompressible Flow," *Journal of Computational Physics*, Vol. 1, No. 1, Academic Press, New York, Aug. **1966**, pp. 119–143.

Bryan, K., "A Scheme for Numerical Integration of the Equations of Motion on an Irregular Grid Free of Nonlinear Instability," *Monthly Weather Review*, Vol. 94, No. 1, Jan. **1966**, pp. 39–40.

Gates, W. L., and Riegel, C. A., "A Study of Numerical Errors in the Integration of Barotropic Flow on a Spherical Grid," *Journal of Geophysical Research*, Vol. 67, No. 2, Feb. **1962**, pp. 773–784.

Grammeltvedt, A., "A Survey of Finite-Difference Schemes for the Primitive Equations for a Barotropic Fluid," *Monthly Weather Review*, Vol. 97, No. 5, May **1969**, pp. 384–404.

Grimmer, M., and Shaw, D. B., "Energy-Preserving Integrations of the Primitive Equations on the Sphere," *Quarterly Journal of the Royal Meteorological Society*, Vol. 93, No. 397, July **1967**, pp. 337–349.

Kurihara, Y., and Holloway, J. L., Jr., "Numerical Integration of a Nine-Level Global Primitive Equation Model Formulated by the Box Method," *Monthly Weather Review*, Vol. 95, No. 8, Aug. **1967**, pp. 509–530.

Lorenz, E. N., "Energy and Numerical Weather Prediction," *Tellus*, Vol. 12, No. 4, Nov. **1960**, pp. 364–373.

Lorenz, E. N., "Persistence of Atmospheric Circulation," *Progress Report* No. 2, Contract Cwb-11392, Massachusetts Institute of Technology, Cambridge, June **1967**, 10 pp.

Masuda, Y., "A Finite Difference Scheme for Making Use of Hexagonal Mesh-Points," paper presented at the WMO/IUGG Symposium on Numerical Weather Prediction, Tokyo, Nov. 26–Dec. 4, **1968**.

Sadourny, R., Arakawa, A., and Mintz, Y., "Integration of the Nondivergent Barotropic Vorticity Equation With an Icosahedral-Hexagonal Grid for the Sphere," *Monthly Weather Review*, Vol. 96, No. 6, June **1968**, pp. 351–356.

Shuman, F. G., "Numerical Experiments With the Primitive Equations," *Proceedings of the International Symposium on Numerical Weather Prediction, Tokyo, November 1960*, Meteorological Society of Japan, Tokyo, Mar. **1962**, pp. 85–107.

Vestine, E. H., Sibley, W. L., Kern, J. W., and Carlstedt, J. L., "Integral and Spherical-Harmonic Analyses of the Geomagnetic Field for 1955.0, Part 2," *Journal of Geomagnetism and Geoelectricity*, Vol. 15, No. 2, **1963**, pp. 73–89.

Williamson, D., "Integration of the Barotropic Vorticity Equation on a Spherical Geodesic Grid," *Tellus*, Vol. 20, No. 4, Nov. **1968**, pp. 642–653.

Winslow, A. M., "Numerical Solution of the Quasilinear Poisson Equation in a Nonuniform Triangle Mesh," *Journal of Computational Physics*, Vol. 1, No. 2, Academic Press, New York, Nov. **1966**, pp. 144–172.

[*Received March 26, 1969; revised May 14, 1969*]